

Cell Reports, Volume 30

## Supplemental Information

### **Chromatin-Binding Protein PHF6 Regulates Activity-Dependent Transcriptional Networks to Promote Hunger Response**

**Linhua Gan, Jingjing Sun, Shuo Yang, Xiaocui Zhang, Wu Chen, Yiyu Sun, Xiaohua Wu, Cheng Cheng, Jing Yuan, Anan Li, Mark A. Corbett, Mathew P. Dixon, Tim Thomas, Anne K. Voss, Jozef Gécz, Guang-Zhong Wang, Azad Bonni, Qian Li, and Ju Huang**

Supplemental Figure 1

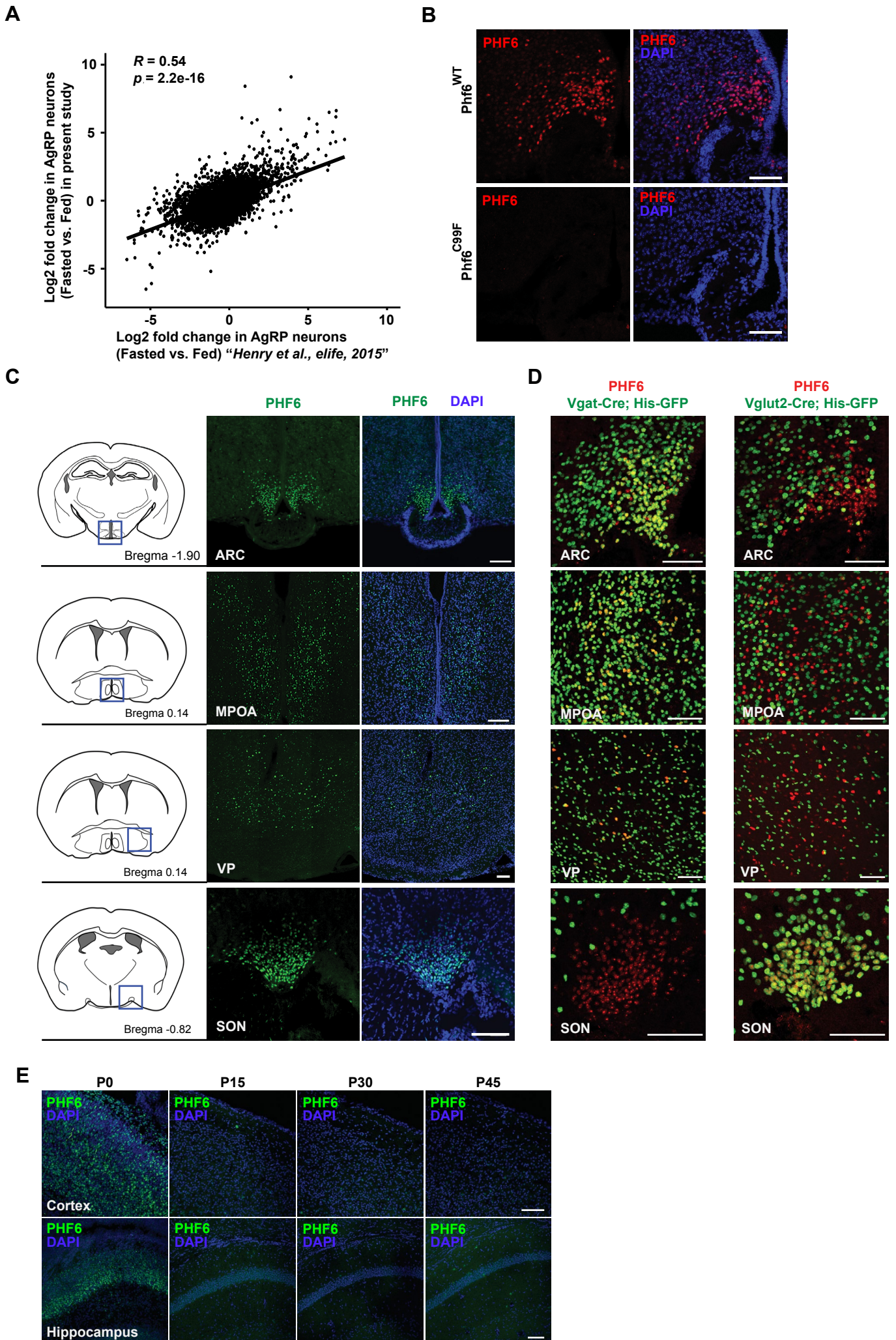
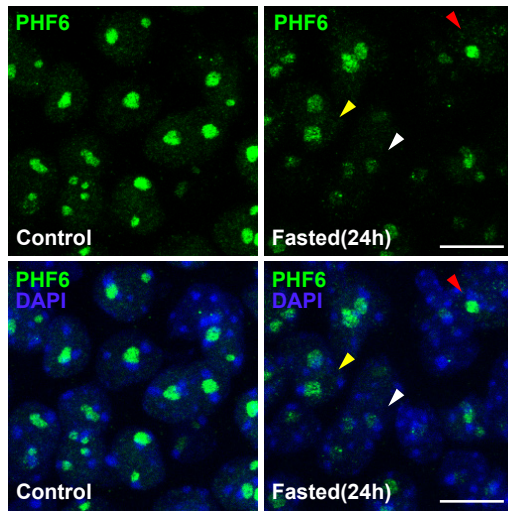


**Figure S1: related to Figure 1.**

**(A)** Positive correlation of the fold changes of gene expression under fasted vs. fed conditions between our experiment and the sequencing data from a previous study (Henry et al., 2015) ( $r = 0.54$  and  $p = 2.2e-16$ ). **(B)** The specificity of PHF6 antibody was validated using PHF6 (C99F) null-mutant mice that lack endogenous PHF6 expression. The scale bars are 75  $\mu\text{m}$ . **(C)** Endogenous PHF6 was detected in four subcortical areas in the adult brain including the arcuate nucleus (ARC), median preoptic area (mPOA), ventral pallidum (VP) and supraoptic nucleus (SON). The scale bars are 100  $\mu\text{m}$ . **(D)** Immunofluorescence of PHF6 in the ARC, mPOA, VP and SON from P26 Vgat-Cre; Histone-GFP and Vglut2-Cre; Histone-GFP mice, in which GABAergic and glutamatergic neurons were labeled with histone conjugated GFP respectively. The scale bars are 75  $\mu\text{m}$ . **(E)** Immunofluorescence of PHF6 in the cortex and hippocampus (CA1) in wild-type mice of age P0, P15, P30, and P45. The scale bars are 75  $\mu\text{m}$ .

## Supplemental Figure 2

**A**



**B**

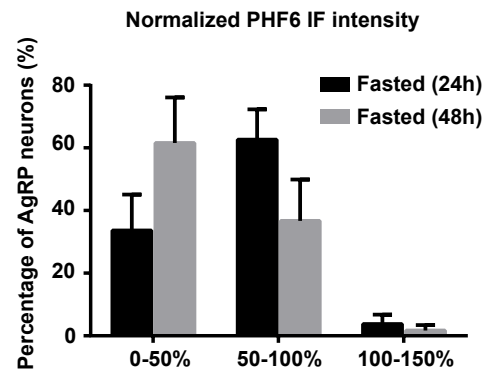


**Figure S2: related to Figure 2.**

**(A)** PHF6 immunohistochemistry in single AgRP neurons in the control and 24-hour fasted conditions. Yellow and white arrowheads indicate representative neurons whose PHF6 immunofluorescence intensity were decreased less than 50% and more than 50% of the average level in the control conditions, respectively. Red arrowhead indicates example of no decrease in PHF6 immunofluorescence intensity. The scale bars are 10  $\mu$ m.

**(B)** Distribution of PHF6 immunofluorescence intensity levels in single AgRP neurons. In the 24-hour fasted conditions, 33.6% $\pm$ 11.5 AgRP neurons showed >50% downregulation (n= 142 out of 385 neurons from 6 mice), while 62.6% $\pm$ 9.6 AgRP neurons showed <50% downregulation (n= 232 out of 385 neurons from 6 mice); In the 48-hour fasted conditions, 61.6% $\pm$ 14.6 AgRP neurons showed >50% downregulation (n= 232 out of 378 neurons from 6 mice), while 36.7% $\pm$ 13.2 AgRP neurons showed <50% downregulation (n= 140 out of 378 neurons from 6 mice). Data are represented as mean  $\pm$  SEM.

Supplemental Figure 3

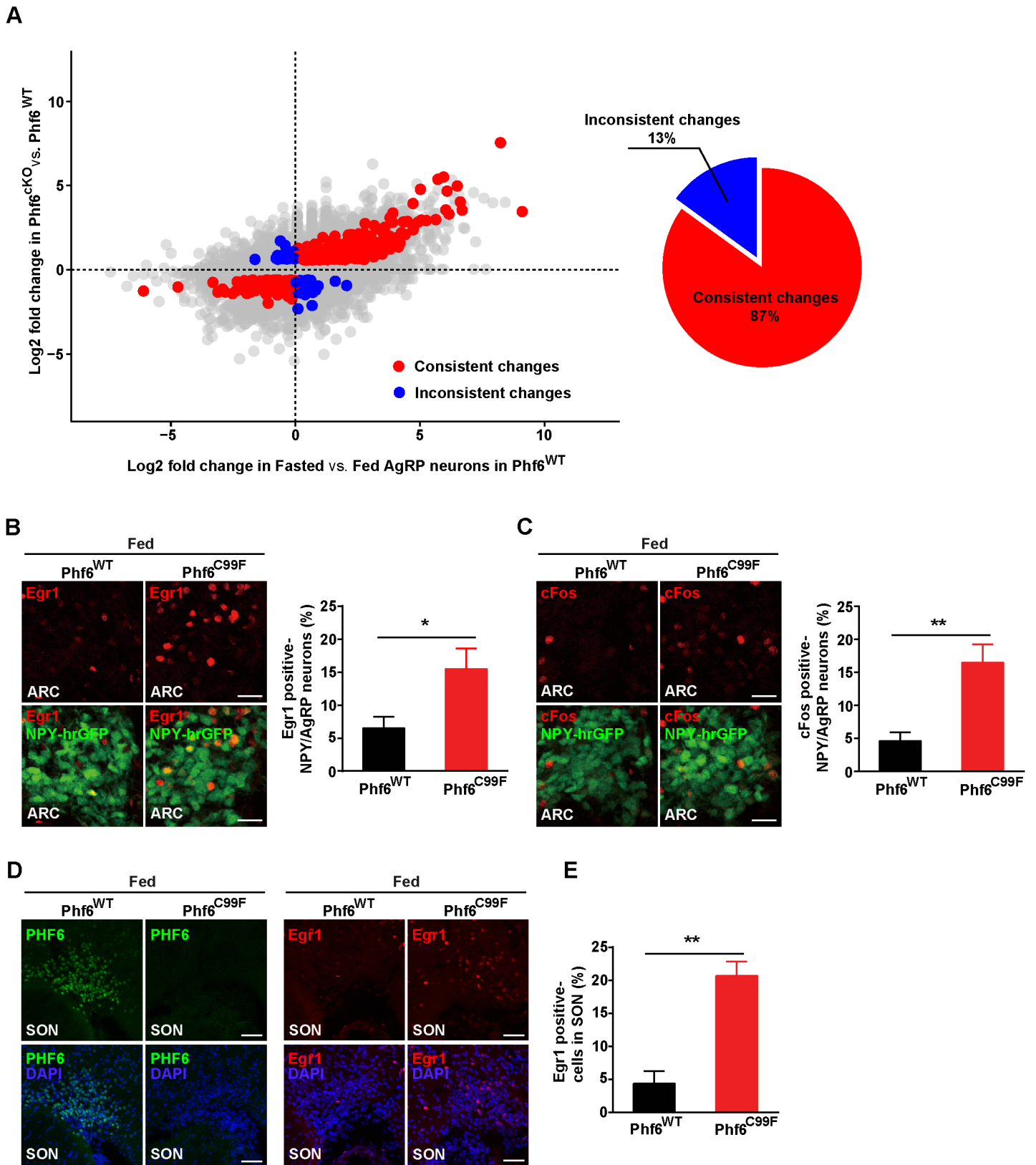
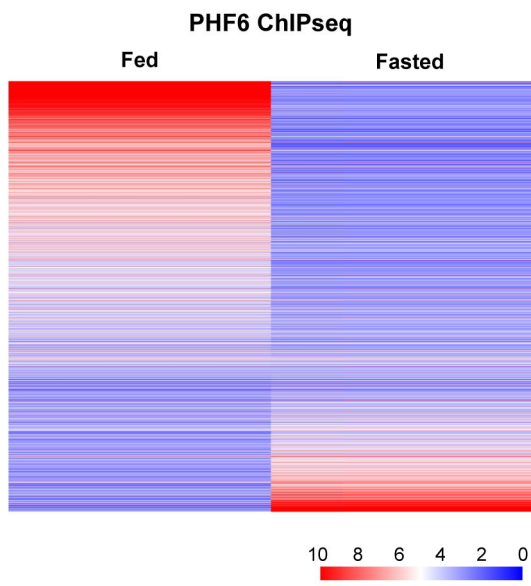


**Figure S3: related to Figure 3.**

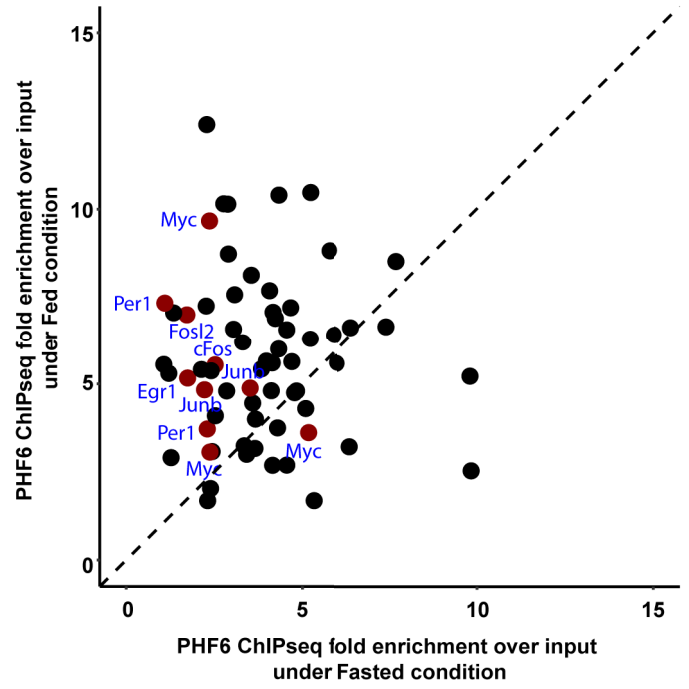
**(A)** Scatter plot showing genes with consistent or inconsistent trends between changes in Phf6<sup>CKO</sup>-fed vs. Phf6<sup>WT</sup>-fed (y axis) and changes in Phf6<sup>WT</sup>-fasted vs. Phf6<sup>WT</sup>-fed (x axis). Among the 421 differentially expressed genes identified in Phf6<sup>WT</sup>-fasted vs. Phf6<sup>WT</sup>-fed, 55 genes showed the opposite trend (blue dots, 13%) and 366 genes showed the same trend (red dots, 87%). **(B)** Immunohistochemistry of Egr1 and the percentage of Egr1-positive NPY/AgRP neurons in Phf6 C99F null-mutant mice and littermate wild-type mice under fed conditions (n=4 for Phf6<sup>WT</sup> mice, n=4 for Phf6<sup>C99F</sup> mice) ( $p < 0.05$ ). The scale bars are 25  $\mu\text{m}$ . **(C)** Immunohistochemistry of cFos and the percentage of cFos-positive NPY/AgRP neurons in Phf6 C99F null-mutant mice and littermate wild-type mice under fed conditions (n=5 for Phf6<sup>WT</sup> mice, n=5 for Phf6<sup>C99F</sup> mice) ( $p < 0.01$ ). The scale bars are 25  $\mu\text{m}$ . **(D, E)** In the Phf6 C99F null-mutant mice, Phf6 depletion led to a higher percentage of Egr1-positive cells in the SON under fed conditions (n=3 for Phf6<sup>WT</sup> mice, n=3 for Phf6<sup>C99F</sup> mice) ( $p < 0.01$ ). The scale bars are 50  $\mu\text{m}$  in (D). Data are represented as mean  $\pm$  SEM.

# Supplemental Figure 4

**A**



**B**



**C**

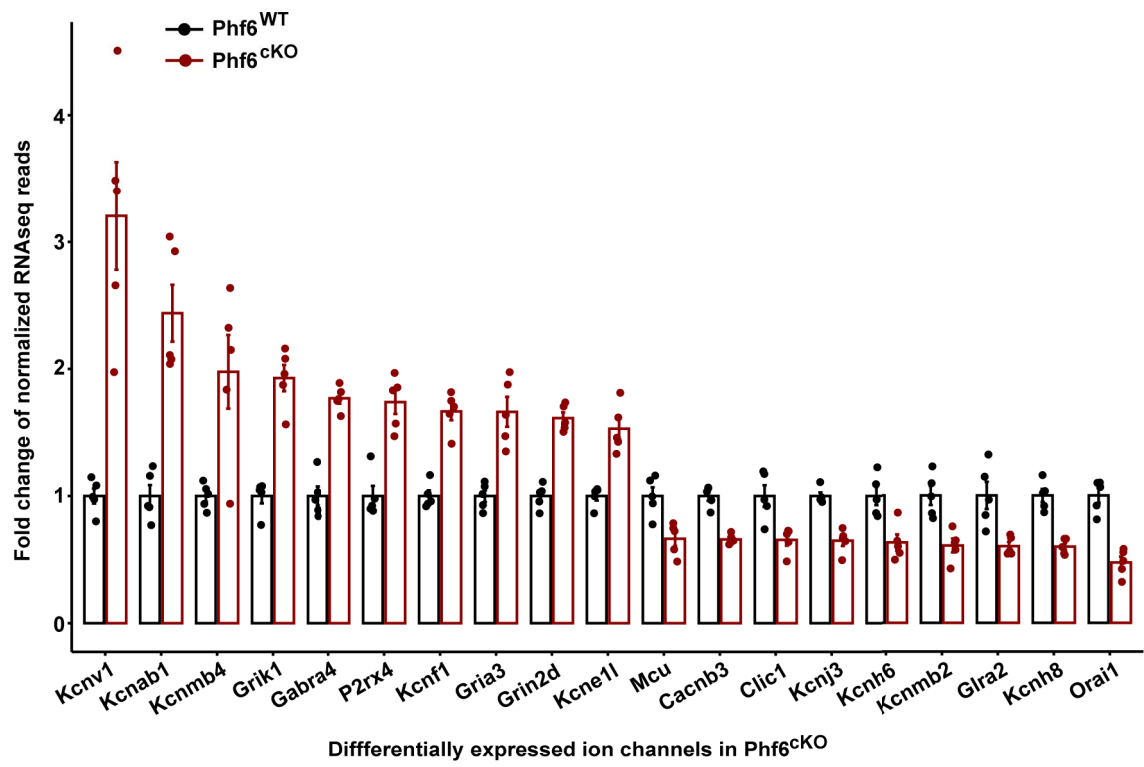
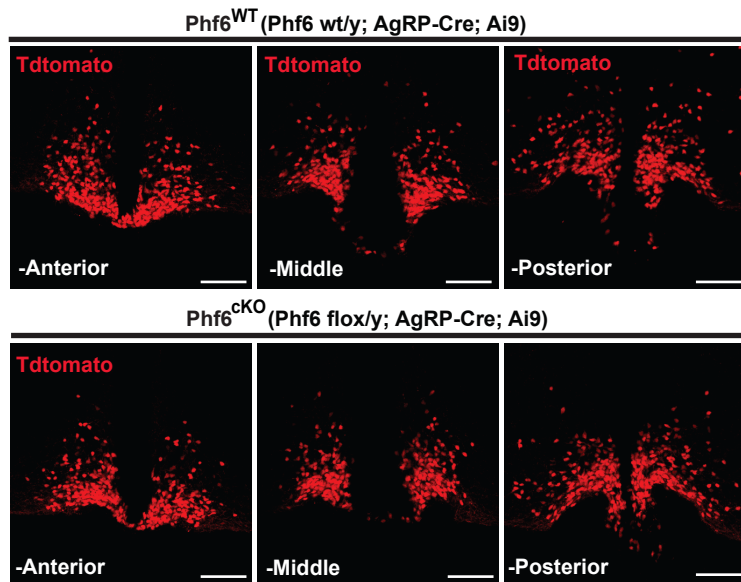


**Figure S4: related to Figure 4.**

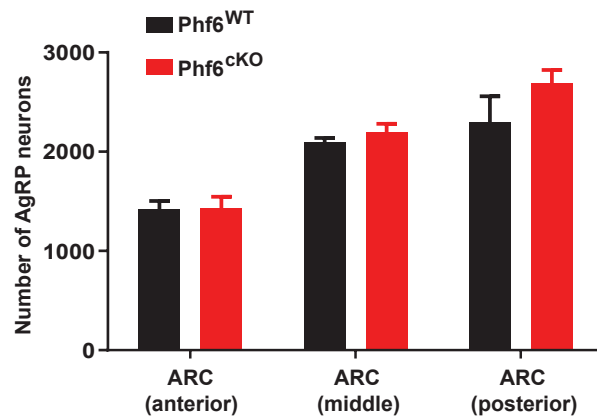
(A) Heatmap plot of the normalized PHF6 ChIPseq reads under fed and fasted conditions. The heatmap illustrated 1269 overlapping PHF6-binding sites under both fed and fasted conditions. Most of them displayed reduced PHF6 occupancy levels in fasted condition compared to in fed condition. (B) Scatter plot of the normalized PHF6 ChIPseq reads close the IEG promoter regions under fed and fasted conditions. The dark red dots represent PHF6-binding peaks near genes encoding *Egr1*, *cFos*, *Fosl2*, *Junb*, *Per1*, and *Myc*. (C) Fold changes in the normalized counts of RNAseq reads for the differentially expressed genes encoding ion channels in *Phf6*<sup>CKO</sup> AgRP neurons. These changes passed the threshold of FDR ( $p$  adj)  $< 0.05$ , fold change  $> 1.5$  or  $< 0.67$ , mean of normalized counts  $\geq 20$ . Data are represented as mean  $\pm$  SEM.

# Supplemental Figure 5

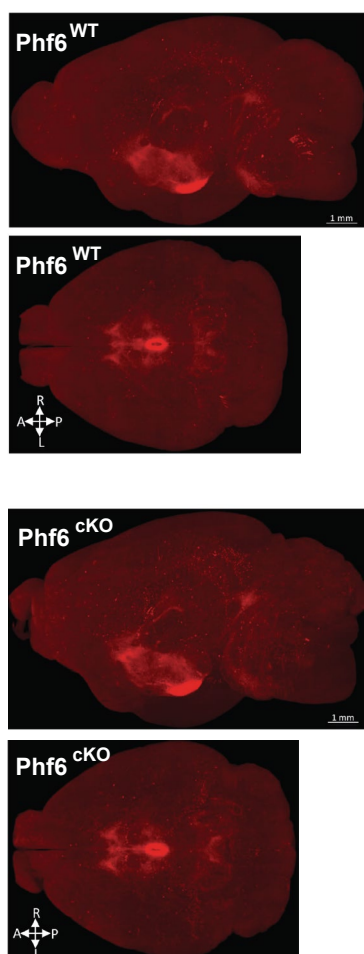
**A**



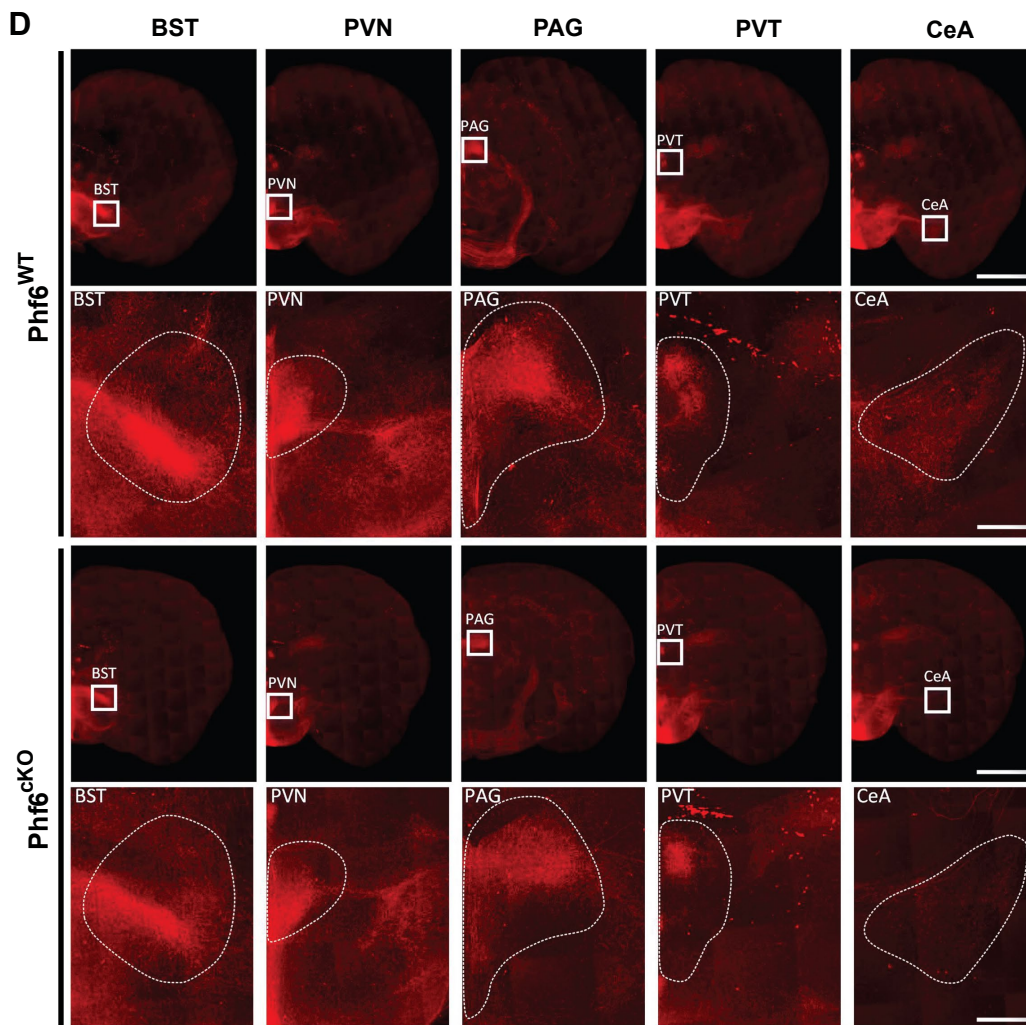
**B**



**C**



**D**



**E**

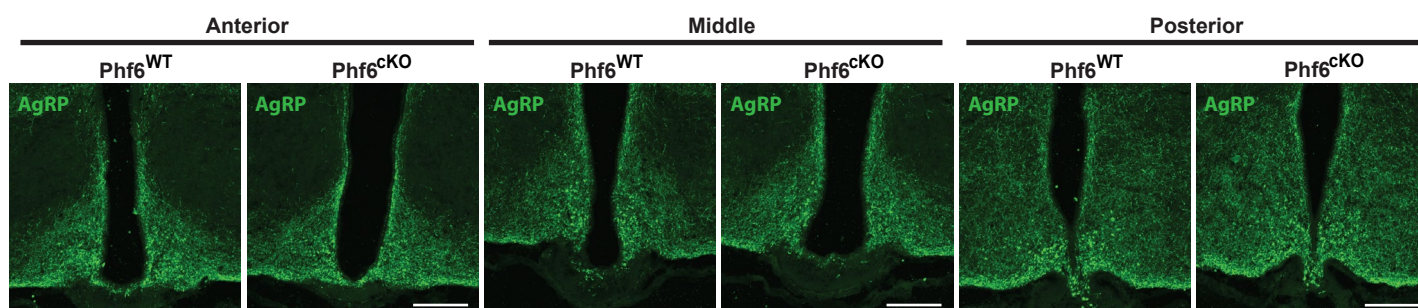


**Figure S5: related to Figure 5.**

**(A)** TdTomato positive AgRP neurons in the continuous sections of the ARC from Phf6<sup>WT</sup> mice (Phf6 wt/y; AgRP-Cre; Ai9) and Phf6<sup>CKO</sup> mice (Phf6 flox/y; AgRP-Cre; Ai9) were counted and calculated. The scale bars are 100  $\mu$ m. **(B)** Quantification of the number of AgRP neurons within the anterior, middle, and posterior part of the ARC from Phf6<sup>WT</sup> mice (n=3) and Phf6<sup>CKO</sup> mice (n=3). Loss of Phf6 had little or no effect on the number of AgRP neurons ( $p = 0.99, 0.36, 0.27$  for anterior, middle, and posterior ARC, respectively). **(C, D)** Whole-brain mapping of AgRP axons by fMOST technique. AgRP neurons in Phf6<sup>WT</sup> mice (Phf6 wt/y; AgRP-Cre; Ai9) and Phf6<sup>CKO</sup> mice (Phf6 flox/y; AgRP-Cre; Ai9) were labeled by tdTomato. Gross axon projection patterns of AgRP neurons were not altered in Phf6<sup>CKO</sup> mice compared to Phf6<sup>WT</sup> mice **(C)**. A slight difference in the axon projection to the PVT and CeA regions in Phf6<sup>CKO</sup> mice were observed **(D)**. The scale bars are 1 mm in (C), 1 mm in the first and third lanes of (D), 200  $\mu$ m in the second and fourth lanes of (D). **(E)** Immunofluorescence of endogenous AgRP in the anterior, middle and posterior part of the ARC. Similar endogenous AgRP protein levels were observed in Phf6<sup>WT</sup> (n=3) and Phf6<sup>CKO</sup> (n=4) mice in fed conditions. The scale bars are 200  $\mu$ m. Data are represented as mean  $\pm$  SEM.

# Supplemental Figure 6

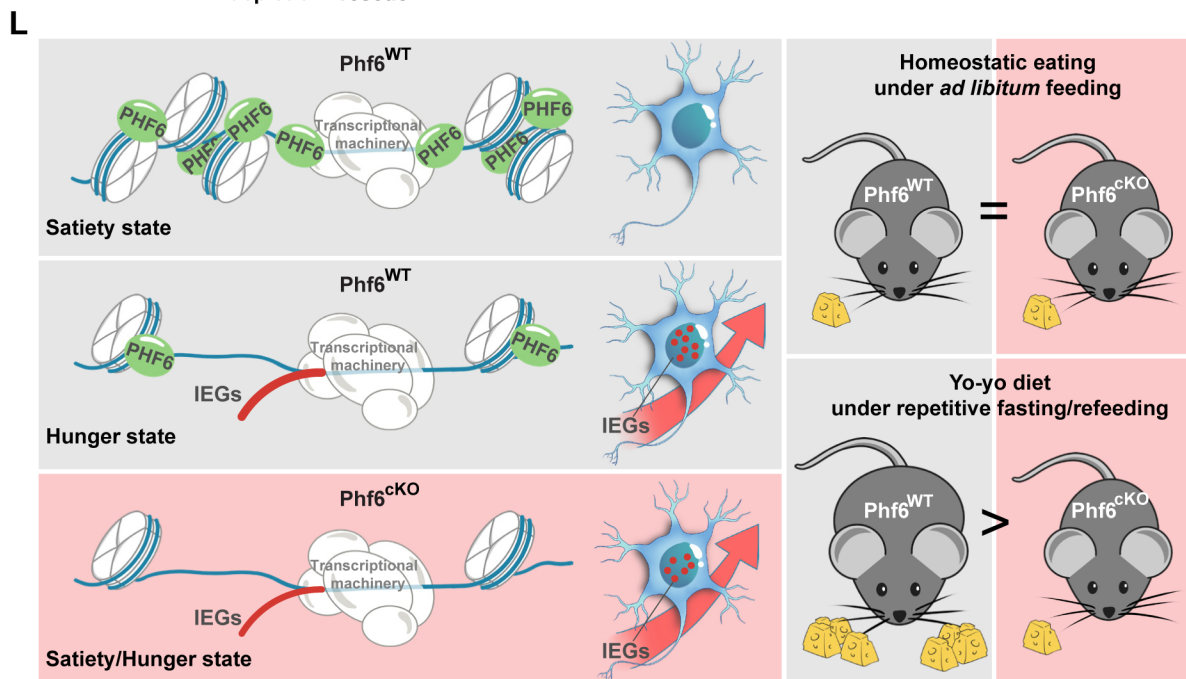
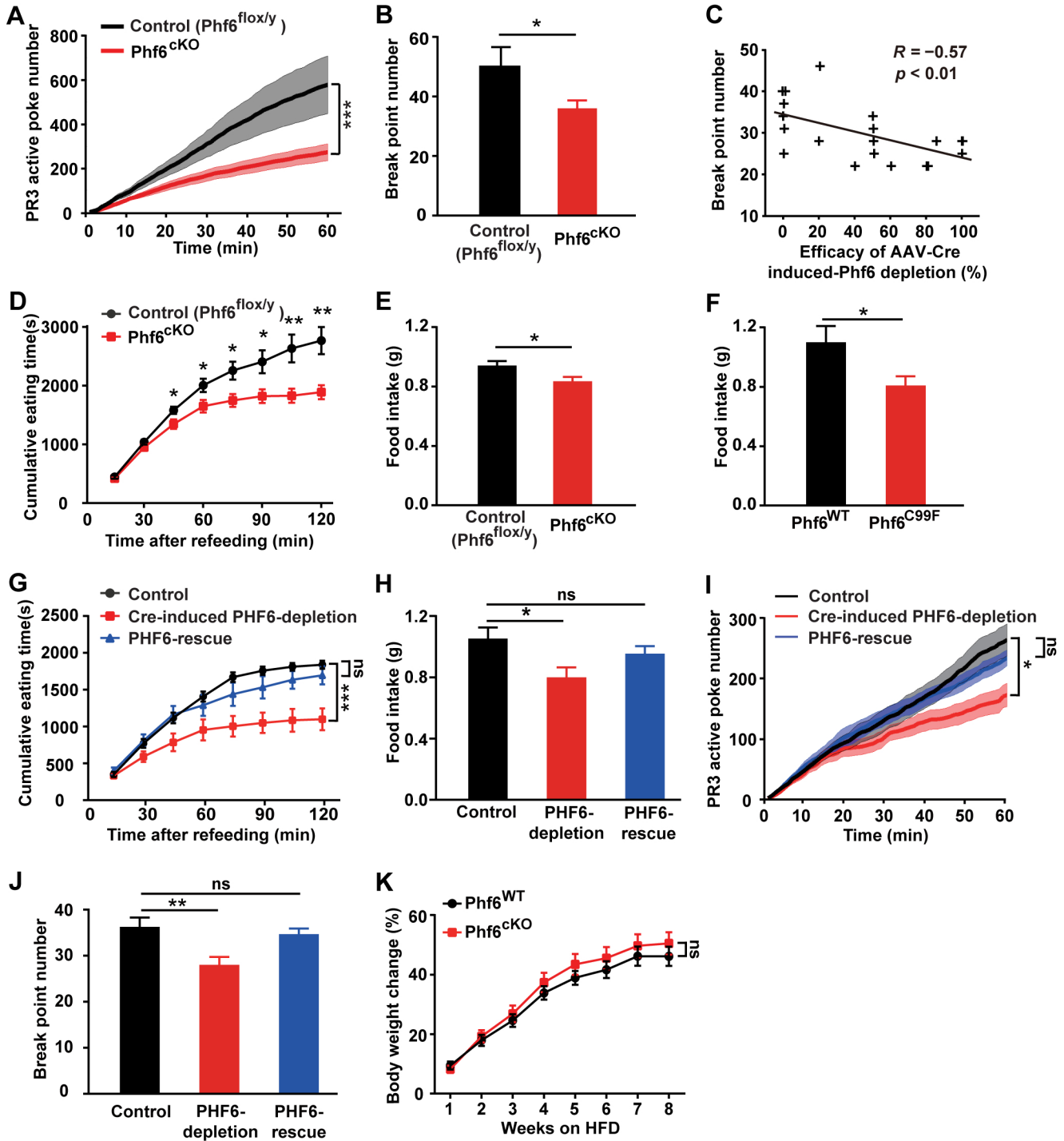


**Figure S6: related to Figure 6.**

**(A)** Loss of PHF6 in AgRP neurons significantly decreased the cumulative active poke number in Phf6<sup>ckO</sup> mice (n=16) compared to that in Phf6<sup>lox/y</sup> control mice (n=15) ( $p < 0.001$ ). **(B)** Loss of PHF6 in AgRP neurons significantly decreased the break point in PR3 test in Phf6<sup>ckO</sup> mice (n=16) compared to that in Phf6<sup>lox/y</sup> control mice (n=15) ( $p < 0.05$ ). **(C)** PR3 break point number was negatively correlated with Phf6 depletion efficacy by AAV-Cre (n=14) ( $R=-0.57$ ,  $p < 0.01$ ). The data at 0 of the x-axis were from the control group by AAV-GFP (n=6). **(D)** Loss of PHF6 in AgRP neurons significantly decreased the cumulative eating time during 2-hour refeeding test after overnight fasting in Phf6<sup>ckO</sup> mice (n=16) compared to that in Phf6<sup>lox/y</sup> control mice (n=16) during the time course from 45 -120 min after the onset of refeeding ( $p < 0.01$ ). **(E)** Amount of food intake during 2-hour refeeding test after overnight fasting was decreased in Phf6<sup>ckO</sup> mice (n=8) compared to that in Phf6<sup>lox/y</sup> control mice (n=8) ( $p < 0.05$ ). **(F)** Amount of food intake during 2-hour refeeding test after overnight fasting was decreased in Phf6<sup>C99F</sup> null-mutant mice (n=13) compared to that in Phf6<sup>WT</sup> control mice (n=11) ( $p < 0.05$ ). **(G, H)** In the 2-hour refeeding test, expression of exogenous PHF6 in the PHF6-deficient mice reversed the cumulative eating time **(G)** and the amount of food intake **(H)** to the levels as those in the control mice. AAV-CMVbG1-EGFP viral injection referred to as “Control”; Combination of AAV-CMVbG1-Cre-EGFP and AAV-EF1a-DIO-EGFP viral injection referred to as “Cre-induced PHF6-depletion”; Combination of AAV-CMVbG1-Cre-EGFP and AAV-EF1a-DIO-EGFP-2A-PHF6 viral injection referred to as “PHF6-rescue” (n=8 for “Control”; n=8 for “Cre-induced PHF6-depletion”; n=9 for “PHF6-rescue”). **(I, J)** In the PR3 test, expression of exogenous PHF6 in the PHF6-deficient mice reversed the cumulative active poke number **(I)** and the break point number **(J)** to the levels as those in the control mice (n=8 for “Control”; n=8 for “Cre-induced PHF6-depletion”; n=9 for “PHF6-rescue”). **(K)** No significant difference was observed in the high fat diet-induced body weight gain between Phf6<sup>WT</sup> mice (n=16) and Phf6<sup>ckO</sup> mice (n=15). **(L)** Model of PHF6 in hunger-driven feeding regulation. The IEG transcription is suppressed by PHF6 in the basal satiety state. Hunger triggers the decrease in PHF6 occupancy from the promoters of IEGs and allows for their rapid induction. Phf6-deficient AgRP neurons constitutively express high levels of IEGs. When the Phf6<sup>ckO</sup> mice are hungry, the Phf6-deficient AgRP neurons cannot further induce robust IEG expression in response to hunger stimulation. Despite unchanged homeostatic eating under normal *ad libitum* feeding conditions, Phf6<sup>ckO</sup> mice display significantly reduced body weight gain on the yo-yo diet under repetitive fasting/refeeding conditions as compared to Phf6<sup>WT</sup> mice. Data are represented as mean  $\pm$  SEM.